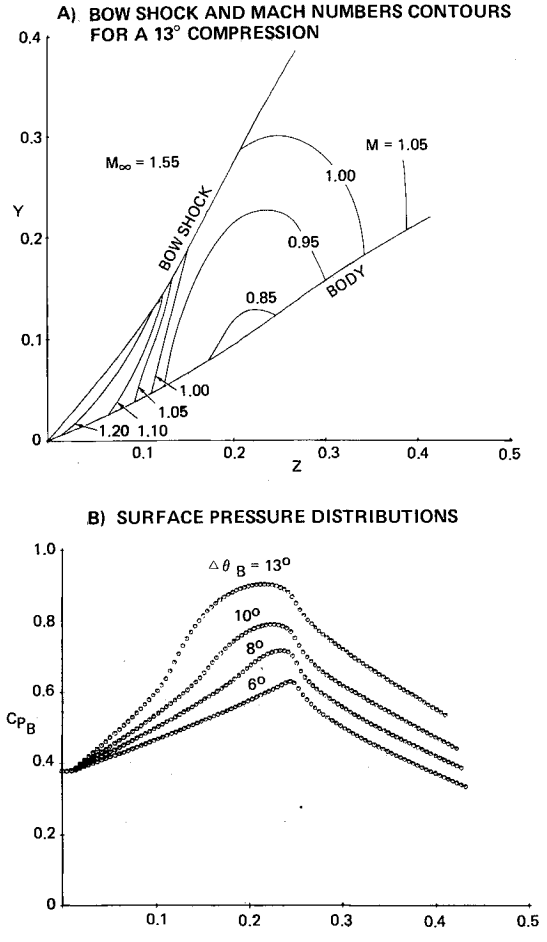

Fig. 2 Axisymmetric solution for a body with a 20-deg supersonic cone at the apex and a gradual compression followed by an expanding afterbody at $M_\infty = 1.55$.

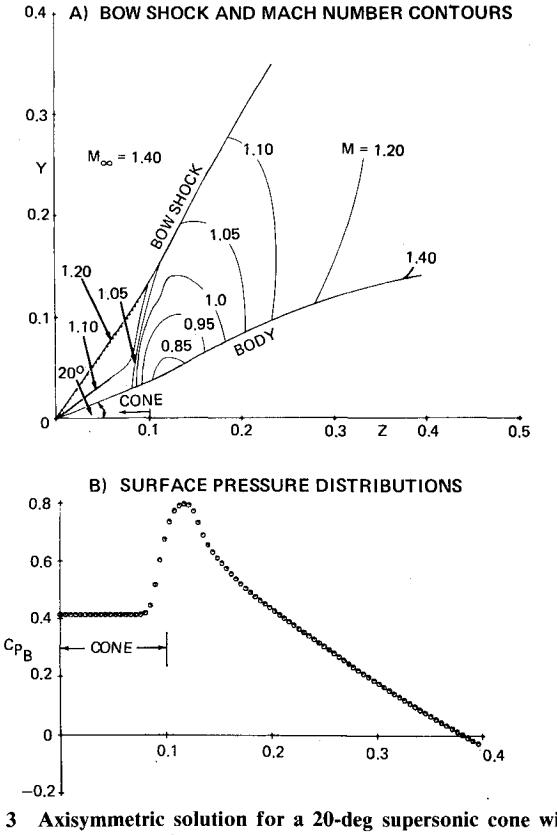

Fig. 3 Axisymmetric solution for a 20-deg supersonic cone with a steep compression of 8 deg followed by an expanding afterbody at $M_\infty = 1.40$.

instabilities were easily eliminated using a continuous switching of the residual with a bias toward the supersonic region. This continuous switching stabilized the downstream sonic line. Figure 2a shows the bow shock and Mach contours for the largest compression of 13 deg. This solution is most interesting because the sonic bubble has intersected the bow shock. The large deflection of the bow shock is already evident. Figure 2b shows the surface pressure distributions for several compression angles. At a compression angle of 6 deg the minimum surface total Mach number is just slightly supersonic. Evidently, the gradual nature of the body deflection leads to a shockless compression on the body surface for the larger compression angles.

Figure 3a shows another Mach contour solution at $M=1.40$ initiated by a 20-deg supersonic cone at the apex, extending to $Z=0.10$, at which point a steep 8-deg compression starts and terminates at $Z=0.13$. An expanding afterbody starts at $Z=0.13$ and terminates in a cylinder at $Z=0.50$. Figure 3b shows the surface pressure distribution on a fine grid of 60×97. The interesting feature of this solution is that the subsonic flow creeps upstream into the supersonic cone region. A shock wave occurs upstream on the cone surface, as indicated by the upstream sonic line attachment position.

Conclusion

A new, efficient, and accurate procedure has been established for computing flows with attached bow shocks at low supersonic freestream Mach numbers that result in embedded subsonic flow regions. This procedure is mesh efficient in that the computation is bounded by a fitted bow shock and hyperbolic upstream and downstream conditions and an iterative procedure need be implemented only in a localized region of subsonic flow.

References

[1] South, J. C., private communication, NASA Langley Research Center, Hampton, Va., 1980.

[2] Shanker, V., Szema, K.Y., and Osher, S., "A Conservative Type-Dependent Full Potential Method for the Treatment of Supersonic Flow with Embedded Subsonic Regions," AIAA Paper 83-1887, July 1983, *Proceedings of AIAA Computational Fluid Dynamics Conference*, pp. 36-47.

[3] Grossman, B., "Numerical Procedure for the Computation of Irrotational Conical Flows," *AIAA Journal*, Vol. 17, Aug. 1979, pp. 828-837.

[4] Grossman, B. and Siclari, M. J., "Nonlinear Supersonic Potential Flow Over Delta Wings," *AIAA Journal*, Vol. 19, May 1981, pp. 573-581.

[5] Siclari, M. J., "Supersonic Nonlinear Potential Flow with Implicit Isentropic Shock Fitting," *AIAA Journal*, Vol. 20, July 1982, pp. 924-932.

[6] Siclari, M. J., "Supersonic Nonlinear Potential Flow with Subsonic Regions and Implicit Isentropic Shock Fitting," AIAA Paper 81-1202, Palo Alto, Calif., June 1981.

[7] Solomon, G. E., "Transonic Flow Past Cone Cylinders," NACA Rept. 1242, 1955.

Nikuradse's Experiment

C.W.B. Grigson*
Marine Consulting, Kristiansand, Norway

Introduction

THE values of the velocity loss term Δu_+ for Nikuradse's sand have been re-evaluated from the original measurements.[1] The wake term has been included in the

Received April 9, 1983; revision received Sept. 15, 1983.

*Consultant.

analysis and corrections made to allow for an error ϵ in the origin of z, the coordinate normal to the surface.

Nikuradse filtered his sand through a sieve, which had only small differences between the pass and retain sizes of the circular holes. Thus, he insured a close uniformity in both the shape and size of the grain. After the sand had been cemented to the pipe, the inner surface was coated with lacquer. Nikuradse's roughnesses may be regarded as quasiregular.

Nikuradse's results have been cited[2] as evidence that the turbulent flow in pipes is different from that in plane geometry, having a Karman constant κ which changes with Reynolds number. The idea that κ is not universal is still put forward. This Note gives an alternative explanation of the results.

The Velocity Profiles

Nikuradse measured velocities at 17 positions along the radius r; for the first $z/r=0$, the next 8 stations run from $z/r=0.02$ to 0.5. Over this region, the semilogarithmic profile is nearly straight. Therefore, the line of least square error was found for these eight points with coordinates $x=\log_{10}(z+\epsilon)$ and $y=u_+$.

In this Note the values $\kappa=0.41$ and $B_0=5.0$ found by Coles[3] are used. The corresponding slope of the line should be $A\ell n10=5.6161$ and ϵ was then found for 23 of Nikuradse's 41 profiles, such that the slope had the value 5.6161 ± 0.0002. Figure 1 shows a set of the corrected velocity profiles when $r/k=126$, where k is the grain size, and Table 1 gives the values of ϵ. In the table, $R_n=2\bar{U}r/\nu$, where $\bar{U}$ is the average velocity and ρ^2 the coefficient of self-determination based on the inner eight points.

Results when $r/k=507$ and 30.6 are similar. The sensitivity of the value deduced for the slope to errors of origin is high: on pipes of 2.474 cm diameter $dA/d\epsilon$ approximately equals $0.006/\mu$m and, on pipes of 9.92 cm diameter $0.0015/\mu$m, where A is the reciprocal of κ. The uncorrected value of $A\ell n10$ occasionally exceeded 5.6161, requiring a negative value of ϵ. This means only that zero errors for the position readings of the probe could be of either sign or that there was a local surface depression at the origin.

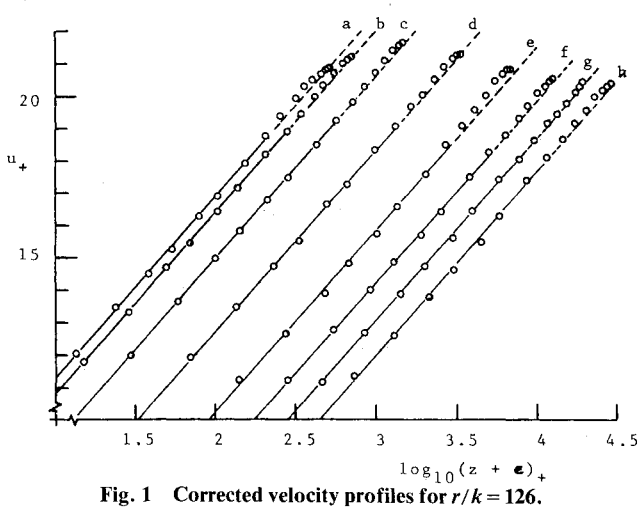

Fig. 1 Corrected velocity profiles for $r/k=126$.

Table 1 Values of ϵ needed to give a slope of 5.6161 when $r/k=126$

Profile	$10^{-3}R_n$	ϵ, μm	ρ^2
a	16.7	82.9	0.9985
b	23.7	24.5	0.9998
c	50.5	11.5	0.9999
d	112	19.0	0.9990
e	231	33.2	0.9969
f	417	150.6	0.9993
g	640	198.6	0.9996
h	960	263.7	0.9981

The need for a correction for the origin seems first to have been realized by Einstein and El Samni.[4] They measured velocity profiles in water flowing over large regular roughnesses. The semilogarithmic profile always had a linear region, but the proper slope was obtained only if a correction for ϵ was made. No probe moves with perfect accuracy along the radius, no pipes are perfectly true and circular, and some error must exist in the origin. In principle, corrections for ϵ are required whether the surfaces are rough or smooth and whether the geometry is tubular or plane.

The profiles all show a wake term clearly. If it is not taken into account, too high a slope will be estimated for the profile. The high value $A\ell n10=5.75$ obtained by Nikuradse can be attributed to 1) the inclusion of all the data from the wake region and 2) the fact that no correction for ϵ was made. Because the sensitivity of the slopes to small errors in the origin is so high, a correction for ϵ should always be made. It follows that the value of the Karman constant cannot be determined with precision from the slope of the logarithmic part of the velocity profile: to find κ, ϵ must be known and to find ϵ, κ must be known.

Δu_+ for Nikuradse's Sand

The velocity profile may be written in the form

$$\Delta u_+ = A\ell nz_+ + B_0 + \phi - \Delta u_+ \tag{1}$$

where the first three terms are the same whether the surface is rough or smooth and all the effects of roughness are included in Δu_+. ϕ is the wake term in Eq. (1) and within the viscous sublayer the difference between the true profile and Eq. (1) is ignored. Coles' original approximation[5] is used for ϕ. On integrating from the surface to the centerline, one obtains

$$\bar{U}/u_\tau = A\ell nru_\tau/\nu + B_0 + A\Pi(1-4/\pi^2) - 3A/2 - \Delta u_+ \tag{2}$$

The smooth case is given when $\Delta u_+=0$. Consider a smooth pipe in which the average discharge $\bar{U}$ is the same as that in a rough pipe of the same bore, so that $\bar{U}_s=\bar{U}_r=\bar{U}$. From Eq. (2), subtracting $\bar{U}_r/u_{\tau r}$ from $\bar{U}_s/u_{\tau s}$, one finds

$$\bar{U}(1/u_{\tau s} - 1/u_{\tau r}) = \Delta u_+ \tag{3}$$

The friction velocity in the rough case is found from the measured pressure gradients, $\bar{U}_r$ from the measured discharge, and $u_{\tau s}$ from the smooth case. Hence, Δu_+ may be found as a function of k_+. Δu_+ cannot become negative, so the three constant terms in Eq. (2) must be large enough to

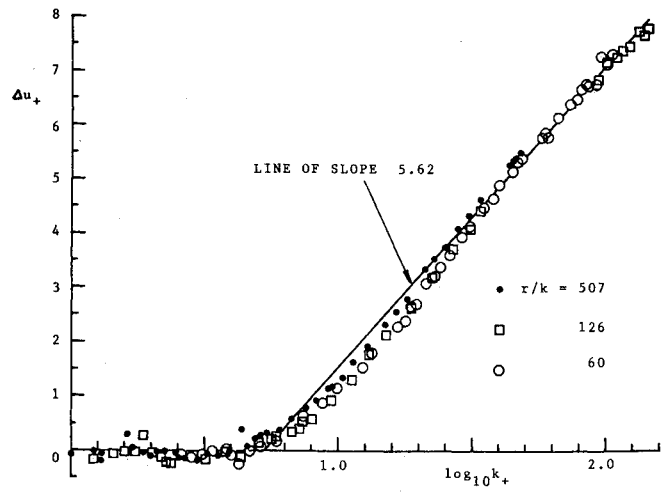

Fig. 2 Dimensionless velocity drop for Nikuradse's sand.

insure this; hence, if $B_0 = 5.0$ the wake strength parameter Π must equal 0.35 (see Fig. 2), which shows Δu_+. Note the excellence of Nikuradse's data. At values of $k_+ > 40$, the curve tends well to the line of slope 5.616. Evidently, if data for smooth pipes with the same bore and discharge rates as those of the rough pipes had been available, κ could have been found from measurements of the discharge rate and pressure gradient alone.

Discussion

Hinze (Ref. 2, p. 718) suggests that the constant A in $u_+ = A\ell nz_+ + B$ varies with R_n in the case of pipes: "Not withstanding the great scatter of the data a trend of the values of A and B as a function of R_n appeared noticeable. The general trend of the parameter A is to increase with increasing R_n for both smooth and rough pipes, with a tendency to level off at $R_n = 10^6$."

Tennekes and Lumley (Ref. 6, p. 176) also suggest that A in a pipe increases at large Reynolds numbers toward a limiting value of three. Their experimental data reach values of ru_τ/ν of 5×10^5, corresponding with Colebrook's measurements on the penstocks of the Niagara Falls power station. Yet a reanalysis of Colebrook's measurements[7] up to $R_n = 3 \times 10^7$ shows that they are consistent with a Coles-type velocity profile with $\kappa = 0.41$.

Hinze's conclusion was based on Nikuradse's pipe work. It is suggested that the trend in A was due to nothing more unusual than that the influence of the wake term and of the inevitable errors in the origin has not been taken into account.

Conclusions

1) Nikuradse's results for pipes coated with sand are consistent with Coles' velocity profile and with the value 0.41 of the Karman constant.

2) Nikuradse's measurements on rough pipes give no evidence for a Karman constant that varies with Reynolds number.

3) Accurate values of the Karman constant cannot be determined from the slope of the logarithmic part of the velocity profile since there is no independent way to find the errors of origin.

Acknowledgments

Dr. A.K. Lewkowicz of Liverpool University and Dr. A.J. Musker of the Admiralty Marine Technology Establishment, Haslar, England, are warmly thanked for valuable discussions.

References

[1] Nikuradse, J., "Laws of Flow in Rough Pipes," NACA TM 1292.

[2] Hinze, J.O., *Turbulence,* 2nd Ed., McGraw Hill Book Co., New York, 1975.

[3] Coles, D., *The Young Person's Guide to the Data,* Vol. II, AFOSR-IFP Stanford Conference on the Calculation of Turbulent Boundary Layers, 1968.

[4] Einstein, H.A. and El-Samni, El-S.A., "Hydrodynamic Forces on a Rough Wall," *Reviews of Modern Physics,* Vol. 21, 1949, pp. 550-524.

[5] Coles, D., "The Law of the Wake in the Turbulent Boundary Layer," *Journal of Fluid Mechanics,* Vol. 1, 1956, pp. 191-226.

[6] Tennekes, H. and Lumley, J.L., *A First Course in Turbulence,* MIT Press, Cambridge, Mass., 1972.

[7] Grigson, C.W.B., "The Drag Coefficients of a Range of Ship Surfaces, II," published for written discussion by the Royal Institute of Naval Architects, London, Paper W4, 1982.

Prediction of Transonic Separated Flows

C. C. Horstman* and D. A. Johnson†
NASA Ames Research Center
Moffett Field, California

Introduction

ALTHOUGH considerable advances have been made in the prediction of the flow over supercritical airfoils, the accuracy deteriorates as the shock wave becomes stronger and eventually separates the boundary layer with increasing angle of attack or Mach number. A recent investigation by the authors[1] provided a detailed comparison between a thoroughly documented transonic flow with shock-induced separations and solutions of the flow using the Navier-Stokes equations. Although the overall flowfield was reasonably predicted, there were several deficiencies in the computations; namely, the failure to predict shock location and the proper extent and size of the separation. New experimental data in a larger wind tunnel have been obtained with the same test model for a wider range of freestream Mach numbers. The recent results indicate that the former data were free from wind tunnel wall effects and have caused the authors to re-examine the previous numerical solutions which employed solid wall boundary conditions. Futhermore, the new data provide a more realistic test for the computation method since they provide trends with varying Mach number.

The purpose of this Note is to inform the reader of the new data, to show results of new Navier-Stokes computations using more compatible boundary conditions, and to assess the effects of the turbulence model choice on predicting Mach number trends.

Experiment

The test model described in Ref. 1 consisted of thin-walled cylinder, 15.2 cm o.d., with an axisymmetric circular arc bump attached 61 cm from the cylinder leading edge. The bump had a thichness of 1.9 cm and a chord length c of 20.3 cm. The streamwise distance x referred to in this Note is the distance from the leading edge of the bump. The present data were obtained in the Ames 6×6 ft Supersonic Wind Tunnel, at Mach numbers from 0.4 to 0.925, at a unit Reynolds number of $10^7 m^{-1}$. The data obtained included surface pressure distributions from the midpoint of the bump aft, boundary-layer separation and reattachment locations using surface oil smear and oil dot techniques, and limited LDV profile data at the trailing edge of the bump.

Computations

The partial differential equations used to describe the mean flowfield are the time-dependent, Reynolds averaged, Navier-Stokes equations for axisymmetric flow of a compressible fluid. For the turbulence closure, the algebraic Cebeci-Smith[2] and the two-equation k-ϵ[3] turbulence models were used. A longitudinal curvature correction[4] was used with the k-ϵ model to determine whether its inclusion could improve the results. The numerical procedure used is the basic explicit second-order, predictor-corrector finite difference method of

Received Aug. 26, 1983; revision received Oct. 11,1983. This paper is declared a work of the U.S. Government and therefore is in the public domain.

*Research Scientist. Associate Fellow AIAA.
†Research Scientist. Member AIAA.